

Chapter 5

Control of Pore Size and Porosity in Lotus-Type Porous Metals

Abstract The porous metals with directional elongated pores are characterized by three important parameters: the pore direction, pore size, and porosity. The pore direction can be adjusted by changing the direction of unidirectional solidification as shown before. Here we describe the way how to control the pore size and the porosity by adjusting the solidification velocity and ambient gas pressure and by addition of oxide particles.

Keywords Boyle's law • Gas pressure • Moisture • Pore size • Solidification velocity

5.1 Control of Pore Size by Solidification Velocity

The lotus copper was fabricated with the mold casting technique by the vacuum-assisted and pressurized casting apparatus consisting of a graphite crucible with a hole on the bottom of the crucible, a stopper stick for preventing the melt flow through the hole, an induction heating coil, and a mold with water-cooled copper plate. High-purity copper was melted in the crucible by radio-frequency heating under high-pressure mixture gas of hydrogen and argon. The molten copper was poured into the mold whose bottom plate was cooled down with water circulated through a chiller. The lateral side of the mold was made of alumina-coated stainless steel tube, which was suitable for insulating in order to be solidified in one direction from the bottom to the top. During the solidification, hydrogen in the melt was rejected at the solid–liquid interface due to the solubility gap of hydrogen between liquid and solid and forms cylindrical pores that were aligned parallel to the solidification direction. The samples were solidified at different solidification velocities through the condition whether a ceramic sheet was inserted between a carbon plate and a copper plate of chiller as shown in Fig. 5.1. R-type thermocouples were inserted in the mold and coupled with a computer-controlled data acquisition system for recording the cooling curves.

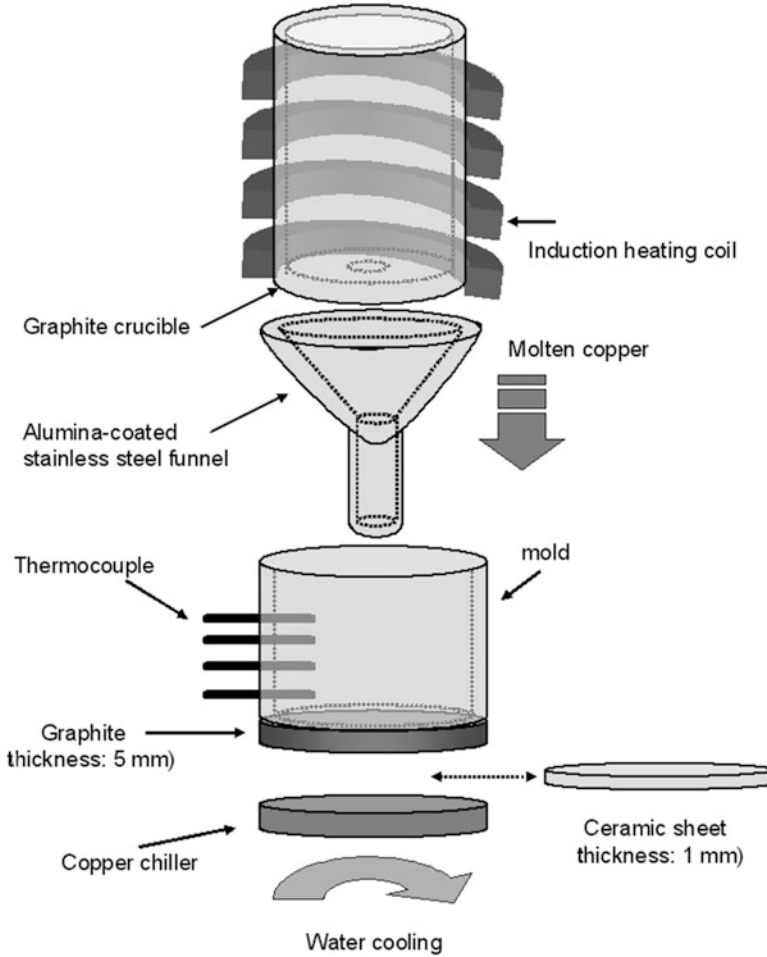


Fig. 5.1 Schematic drawing for measurement of solidification velocity in mold casting technique. The molten metal is dropped through a funnel from the crucible into the bottom mold. Several thermocouples are set up in the vertical direction on the lateral side of the mold. In order to control the solidification velocity, ceramic sheets are inserted between the copper chiller and the mold (Reprinted with permission from [1]. © 2003 Elsevier Ltd)

It is considered that each solidification velocity is constant since the beginning time of solidification linearly increases with increasing distance from bottom of mold, in which the thermal conductivity of copper can be sufficiently high. The samples were solidified with solidification velocities of 1.185 and 0.697 mm s^{-1} through different conditions of the ceramic sheet or not. The optical micrographs of the cross section of the lotus copper are shown in Fig. 5.2. It is apparent that the pore morphology is significantly affected by the solidification velocity. The average

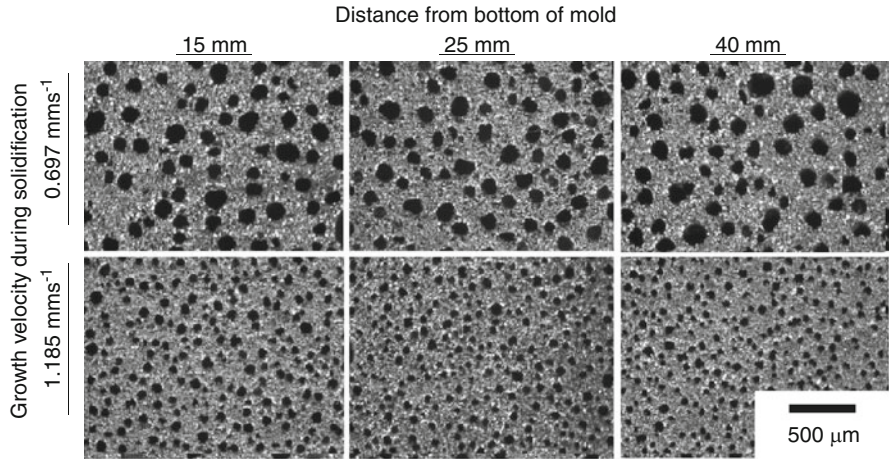


Fig. 5.2 Microstructure of lotus copper in perpendicular section to the solidification direction. Lotus copper ingots were fabricated with two different solidification velocities by the mold casting technique. The micrographs were taken in the sections at the position from different distances from the bottom of the mold (Reprinted with permission from [1]. © 2003 Elsevier Ltd)

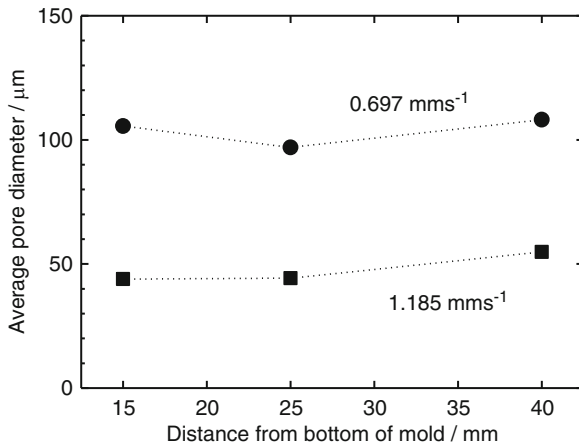


Fig. 5.3 Average pore diameter plotted against distance from the bottom of the mold in lotus copper fabricated by mold casting technique with two different solidification velocities (Reprinted with permission from [1]. © 2003 Elsevier Ltd)

pore diameter is plotted against the distance from the bottom of the mold as shown in Fig. 5.3. The pore diameter in the lotus copper fabricated with the solidification velocity of 0.697 mm s^{-1} is twice larger than that with 1.185 mm s^{-1} . It can be understood that the amount of hydrogen diffusing from liquid to the pores increases with decreasing solidification velocity and then the pores formed with the velocity

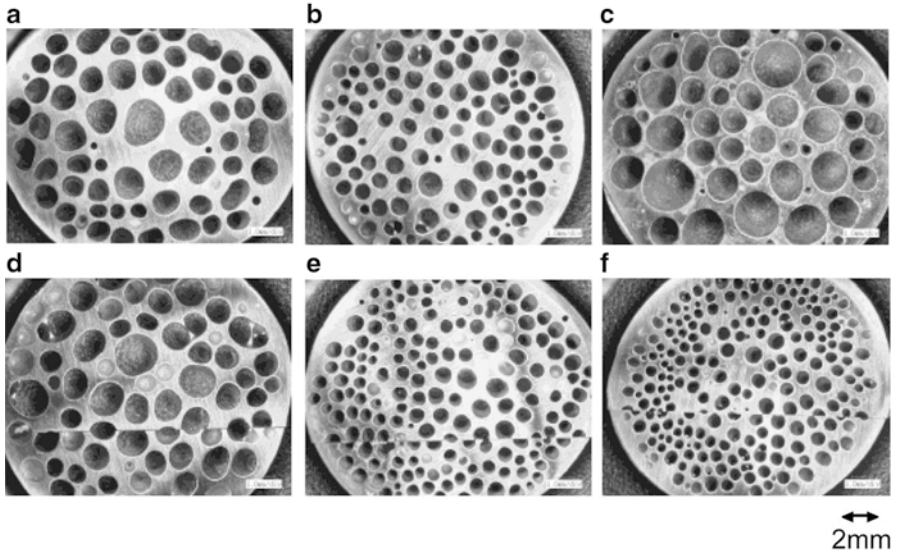


Fig. 5.4 Cross sections perpendicular to the solidification direction of lotus stainless steel fabricated under hydrogen gas of 1.0 MPa by continuous zone melting technique. The upper figures (a), (b), and (c) are of the rods fabricated without gas-blow cooling and the lower figures (d), (e), and (f) are of those fabricated with gas-blow cooling. The transfer velocities are $160 \mu\text{m s}^{-1}$ for (a) and (d), $330 \mu\text{m s}^{-1}$ for (b) and (e), and $500 \mu\text{m s}^{-1}$ for (c) and (f) (Reprinted with permission from [2]. © 2005 The Minerals, Metals & Materials Society and ASM International)

of 0.697 mm s^{-1} become larger than those with 1.185 mm s^{-1} . As the solidification velocity increases, the pore size decreases but the number density of pores increases. Increasing the solidification velocity causes an increase in the hydrogen supersaturation of the solid–liquid interface and then the driving force to nucleate the pores increases. If the entire amount of hydrogen dissolved in the melt is diffused into the pores, the pore size can decrease with increasing number density of pores. Consequently it can be understood that the solidification velocity can affect the average pore diameter of lotus copper [1].

In Fig. 5.4, the cross-sectional planes perpendicular to the solidification direction in lotus stainless steel rods fabricated by the continuous zone melting technique under the hydrogen atmosphere of 1.0 MPa without or with the gas-blow cooling gas are shown. The average pore diameter and porosity determined by image analyses are shown in Table 5.1. The average pore diameter decreases with increasing transfer velocity, while the porosities are not much different. It is found that the cooling rate is almost proportional to the transfer velocity in fabricating porous metal rods with gas-blow cooling. The cause of the smaller pore diameters in the rods fabricated with the larger velocities is considered to be due to the higher cooling rates [2]. Such tendency is consistent with the experimental results in the fabrication

Table 5.1 Porosity and average pore diameter of lotus stainless steel fabricated under hydrogen atmosphere of 1.0 MPa by continuous zone melting technique with/without gas-blow cooling

Transfer velocity ($\mu\text{m s}^{-1}$)	Gas-blow cooling	Porosity (%)	Average pore diameter (μm)
160	×	52	890
330	×	49	710
500	×	64	1,070
160	○	59	1,020
330	○	48	550
550	○	46	480

of porous copper by the casting technique [1]. Furthermore, since the temperature gradient increases by using gas-blower, it is considered that the solidification velocity increases by the gas-blower and thus the pore size becomes smaller.

5.2 Control of Pore Size and Porosity by Ambient Gas Pressure

The average pore diameter and porosity of the lotus stainless steel rods that were fabricated under hydrogen and argon or helium of various pressures with the transfer velocity of $330 \mu\text{m s}^{-1}$ are summarized in Fig. 5.5a, b. The average pore diameter and porosity decrease with increasing pressure under the atmosphere of only hydrogen. The concentration of hydrogen dissolving in liquid metal is proportional to the square root of hydrogen pressure according to Sieverts' law. On the other hand, the volume of gas in the pores is reciprocally proportional to the pressure of the ambient gas according to Boyle's law since the pressure of pores should be almost in balance with the pressure of ambient gas. Therefore, it is considered that the decrease in the average pore diameter and porosity with increase in pressure of hydrogen is caused by more significant influence of pore volumes than that of the solubility of hydrogen.

Under mixed gas of hydrogen and argon of a constant total pressure, the porosity increases and average pore diameter decreases with increasing partial pressure of hydrogen. Hydrogen solubility in the melt of stainless steel increases with increase of the hydrogen pressure according to Sieverts' law. The pores are composed of only hydrogen since argon is not dissolved in the melts. Since the pressure in the pores should be balanced with the total pressure, the pressure in the pores is constant regardless of the variation of the hydrogen partial pressure under a constant total pressure. Therefore, it is considered that the increase in the hydrogen solubility due to the increase of the partial pressure of hydrogen leads to the increase in porosity under a constant total pressure.

Such a pressure dependence of porosity of lotus stainless steel fabricated by the continuous zone melting technique is qualitatively consistent with that of lotus

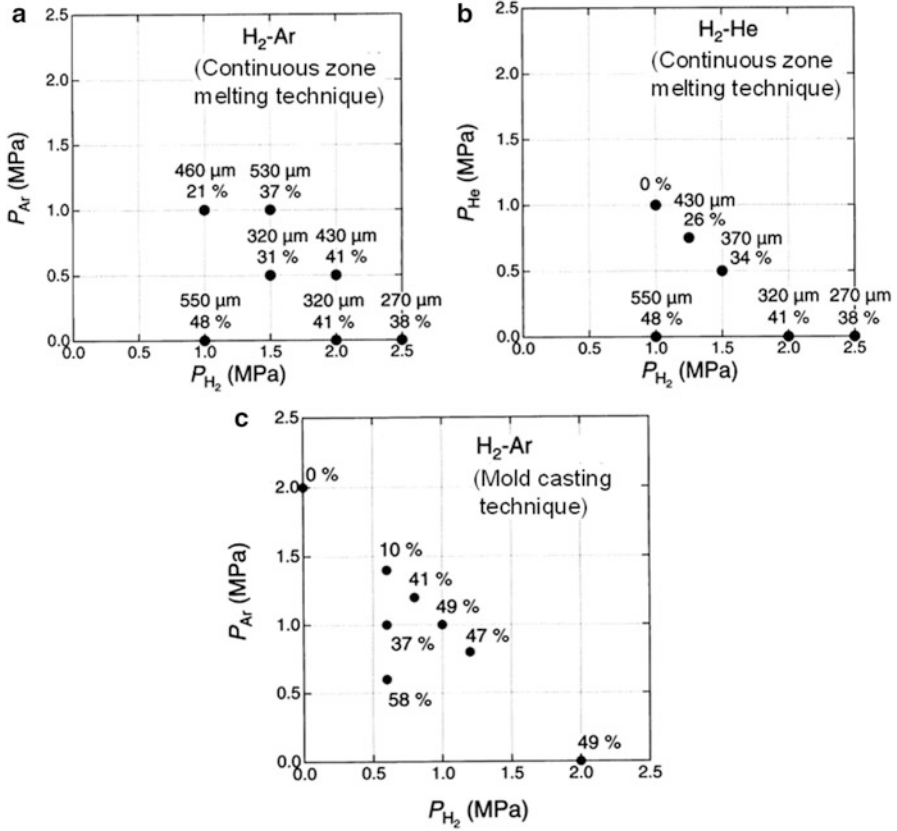


Fig. 5.5 Average pore diameter (upper number) and porosity (lower number) of the lotus stainless steel fabricated by continuous zone melting technique with gas-blowing cooling under various pressures of mixed gases composed of (a) hydrogen and argon or (b) hydrogen and helium. These diagrams are for the cases where the transfer velocity is $330 \mu m s^{-1}$. (c) The porosity of lotus stainless steel fabricated by mold casting technique (Reprinted with permission from [2]. © 2005 The Minerals, Metals & Materials Society and ASM International)

stainless steel fabricated by mold casting technique [3] shown in Fig. 5.5c. However, the porosity by the continuous zone melting technique is a little lower than that by the mold casting technique. It is understood that the hydrogen concentration in the melt zone may not be saturated since the hydrogen in the ambient atmosphere can be dissolved into the melt only while the metal is transferred across the melt zone of at most 10 mm. Therefore, the hydrogen concentration is a little smaller for the continuous zone melting technique. This leads to result in the smaller porosity of the lotus stainless steel fabricated by the continuous zone melting technique than that by the mold casting technique. In Table 5.1, the porosity decreases little by little with increase of the transfer velocity in the case with gas-blow cooling,

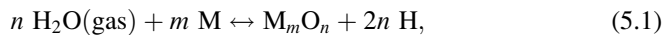
comparing with the case without the cooling. This is also possibly due to the decrease of hydrogen dissolution into melt with increase of the transfer velocity.

On the other hand, the average pore diameter increases with increasing argon pressure under a constant total pressure. This is possibly related with the heat conductivity of ambient gas. The heat conductivity of hydrogen is $21.18 \times 10^{-2} \text{ Wm}^{-1} \text{ K}^{-1}$ (373 K) [4] and that of argon is $2.12 \times 10^{-2} \text{ Wm}^{-1} \text{ K}^{-1}$ (373 K) [4], the latter of which is an order of magnitude lower than that of hydrogen. Therefore, the heat conductivity of ambient gas significantly decreases with increasing partial pressure of argon and hence the efficiency of heat transmission from the metal rod to the ambient gas by gas-blow cooling also decreases. Consequently, this leads to the lowering of the cooling rate and hence to the increase in average pore diameter.

Figure 5.5b shows the pressure dependence of average pore diameter and porosity of the lotus stainless steel fabricated under mixed gas of hydrogen and helium. The porosity decreases with increasing helium pressure under a constant total pressure. This trend is almost consistent with the case where mixed gas of hydrogen and argon is used. The average pore diameter also has a trend of increase with increasing helium pressure. The heat conductivity of helium is $17.77 \times 10^{-2} \text{ Wm}^{-1} \text{ K}^{-1}$ (373 K) [4], which is a little smaller than that of hydrogen but in the same order of magnitude as hydrogen. Therefore, it is expected that the heat conductivity of ambient gas and hence the cooling rate does not much vary by increasing helium partial pressure under a constant total pressure. Nevertheless, the average pore diameter depends on the helium pressure under a constant total pressure similar to the case of hydrogen-argon gas. The reason for this is not very clear at present. Further investigations are required.

5.3 Control of Pore Size by Addition of Oxide Particles

Suematsu et al. proposed a fabrication method of lotus nickel using moisture during the solidification in argon atmosphere [5]. The pore size of the sample fabricated by this method is smaller than that of the sample fabricated in pressurized hydrogen atmosphere (PGM). Such smaller pore formation is attributed to formation of nucleation sites of the oxide. According to the following reaction,



the moisture decomposes into hydrogen and metal oxide. The former produces hydrogen pores, while the latter may serve as the nucleation sites for the pores. Although the moisture could be produced by the reverse reaction (1), the moisture (H_2O) itself cannot be dissolved into the molten nickel. Therefore, it is considered that the moisture does not contribute to evolve any pores in the solidified nickel. The experimental results by Suematsu et al. suggests that the pore size in lotus nickel can be controlled by the amount and/or particle size of NiO powder [5].

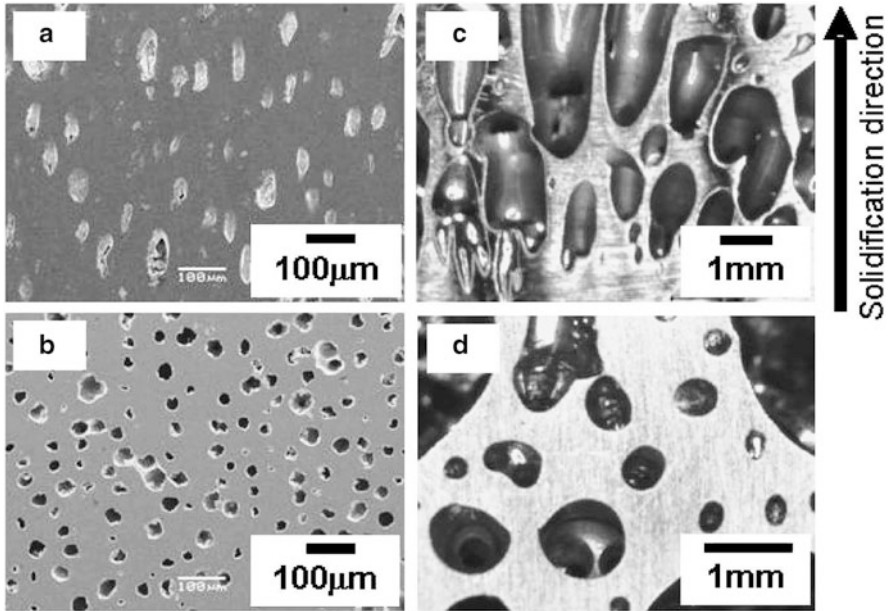


Fig. 5.6 The longitudinal cross-sectional (a) and transversal cross-sectional (b) views of the sample fabricated in mixture gas of 0.65 MPa Ar and 0.15 MPa H₂ using NiO powder whose weight is 0.5 g and particle size is 7 μm. (c) and (d) show the longitudinal cross-sectional and transversal cross-sectional views of the sample fabricated in the same atmosphere without NiO powder (Reprinted with permission from [6]. © 2008 Japan Institute of Metals)

Here the effect of NiO powder on the formation of pores was examined by Onishi et al. in order to elucidate the relation among pore size in lotus nickel, the amount, and particle size of NiO powder [6]. The solidification was conducted by mold casting under pressurized gas of argon and hydrogen. 120 g of nickel ingot with 99.9 % purity was heated in alumina crucible by an induction coil and the molten nickel was poured into the mold whose bottom was made of copper and the side was made by molybdenum. The bottom of the mold was cooled by water chiller. An appropriate amount of NiO powder was put on the copper mold before casting.

Figure 5.6a, b shows the longitudinal and transversal cross-sectional views of the sample fabricated in the mixture of gas 0.65 MPa Ar and 0.15 MPa H₂ using NiO powder whose weight is 0.5 g and particle size is 7 μm. On the other hand, Fig. 5.6c, d shows longitudinal and transversal cross-sectional views of the sample fabricated under the same atmosphere without NiO powder. The porosity and average pore diameter calculated from Fig. 5.6 are 29 % and 31 μm for (b) and 62 % and 427 μm for (d), respectively. Apparently, the average pore diameter for (b) is smaller than that of (d). On the other hand, the aspect ratio of pores for (a), 2.2, is smaller than that of (c), 4.7. When the melt is solidified, supersaturated hydrogen in the solid diffuses into pores. If the number density of pores increases, the amount

Fig. 5.7 Dependence of porosity on amount of NiO powder with different sizes of the particles. Lotus nickel was fabricated in mixture gas of 0.85 MPa Ar and 0.15 MPa H₂ (Reprinted with permission from [6]. © 2008 Japan Institute of Metals)

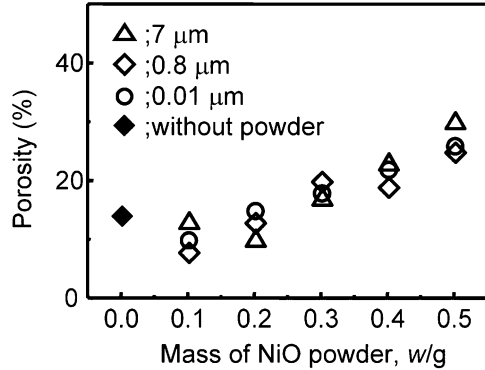
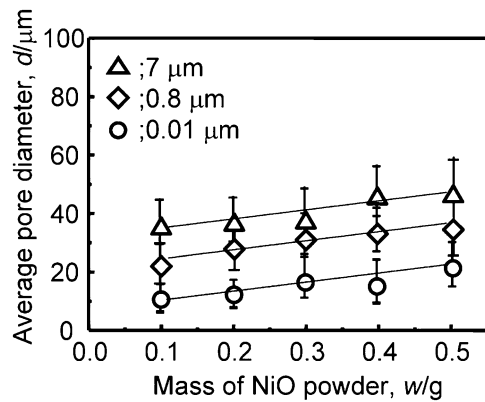


Fig. 5.8 The average pore diameter of the samples as a function of mass of NiO powder with different sizes of the particles. Lotus nickel was fabricated in mixture gas of 0.85 MPa Ar and 0.15 MPa H₂ (Reprinted with permission from [6]. © 2008 Japan Institute of Metals)



of hydrogen which diffuses into each pore from the surrounding region decreases so that the pores cannot grow continuously in the direction of the solidification. Thus, the aspect ratio of the pores in the case of addition of NiO is shorter than that without NiO. Since the pore size decreases and the number of density of pores increases by addition of NiO, it is considered that the oxide powders act as nucleation sites for pores.

Figure 5.7 shows the porosity change with the amount of NiO powder. All samples in Fig. 5.7 were fabricated in the mixture of 0.85 MPa Ar and 0.15 MPa H₂. The porosity increases with increasing amount of NiO powder. It was suggested that about half of the hydrogen amount with the solubility gap between solid and liquid is released to the atmosphere not to contribute to the pore formation [7]. However, if the number of the pore nucleation sites increases by addition of excess NiO powder, more insoluble hydrogen may be trapped by the nucleation sites. Thus, higher porosity was observed with increasing mass of NiO powder, as shown in Fig. 5.7. However, no significant effect of the particles size of NiO powder on the porosity was found.

Figure 5.8 shows the average pore diameter of the samples as a function of the mass of NiO powder. The pore diameter decreases with decreasing particle size of

NiO powder. Since the number density of particles significantly increases with decreasing particle size when the same mass of NiO powder is added, the number of pores increases and the resulting pore size decreases as shown in Fig. 5.8. This may be attributed to the increase in the number of hydrogen atoms for formation of the pores by NiO powder addition. On the other hand, the average pore diameter monotonously increases with increasing amount of NiO powder. It is concluded that NiO powder can serve as nucleation sites for the pore formation in the process of the solidification.

References

1. Hyun SK, Nakajima H (2003) *Mater Lett* 57:3149–3154
2. Ikeda T, Aoki T, Nakajima H (2005) *Metall Mater Trans A* 36A:77–86
3. Ikeda T, Tsukamoto M, Nakajima H (2002) *Mater Trans* 43:2678–2684
4. National Astronomical Observatory (ed) (2002) *Chronological scientific tables*. Maruzen Co. Ltd, Tokyo, p 404
5. Suematsu Y, Hyun SK, Nakajima H (2004) *J Jpn Inst Metals* 68:257–261
6. Onishi H, Ueno S, Nakajima H (2008) *Mater Trans* 49:2670–2672
7. Yamamura S, Shiota H, Murakami K, Nakajima H (2001) *Mater Sci Eng A* 318:137–143